Structural and electronic evolution of the $As(OH)_3$ molecule in high temperature aqueous solutions: An x-ray absorption investigation

Denis Testemale[a)]
Laboratoire de Cristallographie CNRS-Grenoble, UPR5031, 25 avenue des Martyrs, BP 166 38042 Grenoble Cedex 09, France and SNBL/ESRF, 6 rue Jules Horowitz, BP 220 38043 Grenoble

Jean-Louis Hazemann
Laboratoire de Cristallographie CNRS-Grenoble, UPR5031, 25 avenue des Martyrs, BP 166 38042 Grenoble Cedex 09, France

Gleb S. Pokrovski
Laboratoire de Géochimie, UMR 5563, CNRS-OMP-Université Paul Sabatier, 38 rue des 36 Ponts, 31400 Toulouse, France and Institut des Sciences de la Terre d'Orléans (ISTO), UMR6133, 1A rue de la Férollerie, 45071 Orléans Cedex 02, France

Yves Joly
Laboratoire de Cristallographie CNRS-Grenoble, UPR5031, 25 avenue des Martyrs, BP 166 38042 Grenoble Cedex 09, France

Jacques Roux
Institut des Sciences de la Terre d'Orléans (ISTO), UMR6133, 1A rue de la Férollerie, 45071 Orléans Cedex 02, France

Roger Argoud and Olivier Geaymond
Laboratoire de Cristallographie CNRS-Grenoble, UPR5031, 25 avenue des Martyrs, BP 166 38042 Grenoble Cedex 09, France

(Received 5 May 2004; accepted 29 June 2004)

The geometrical and electronic structure of the arsenious acid molecule $As(OH)_3$ in aqueous solutions has been investigated by x-ray absorption spectroscopy (XAS) within extended x-ray absorption spectroscopy (EXAFS) and x-ray absorption near edge structure (XANES), using realistic first-principle calculations in the latter case. This investigation was performed on aqueous solutions of arsenious acid from ambient to supercritical conditions ($P=250$ and 600 bars, $T \leqslant 500\,^{\circ}C$) using a new optical cell. The analysis of the XAS spectra is consistent with (1) a constant As-O distance, (2) an opening of the O-As-O angles within the C_{3V} pyramidal structure in the range 30–200 °C. This structural evolution comes along with a small decrease of the partial charges of the atoms in the $As(OH)_3$ molecule. The explanation invoked for both structural and electronic modifications observed is the weakening of the interactions, through hydrogen bonds, between the $As(OH)_3$ complex and water molecules. This is a fingerprint of the similar weakening of hydrogen bonding interactions in the solvent itself. © *2004 American Institute of Physics.*
[DOI: 10.1063/1.1785150]

I. INTRODUCTION

The understanding of the processes of molecular interactions in fluids at elevated pressures and temperatures is of crucial importance, in particular, in the case of aqueous solutions.[1,2] The growing interest in these processes stems from both the fundamental and applied insights that their understanding brings to the geochemical, (bio)chemical, and industrial communities. It must be emphasized in the case of aqueous solutions that the interparticle interactions under elevated temperature and pressure conditions are very sensitive to the structure of the solvent and, in particular, to the hydrogen bonding strength. As a consequence, studying the structural and electronic evolution of solute particles in aqueous solutions is an efficient indirect method to get information on the solvent itself.

Two situations must be considered: either the solute species are ions or neutral molecules. In the former case, the study of ion hydration-shell structures under high temperature and high pressure conditions gives information on the molecular reorientation taking place in the solvent,[2] and on the evolution of solvent permittivity ϵ that controls coulombic interactions.[3] The present study belongs to the latter case where the solute under consideration is a neutral complex. The molecule of aqueous arsenious acid $As(OH)_3$ is a very good candidate as a probe: it possesses a nonzero dipole moment that may evolve with the solvent permittivity ϵ and three OH groups likely to establish hydrogen bonds with solvent water molecules.

Among different techniques (x-ray diffraction, isotopic substitution neutron scattering, Raman, IR, and NMR spectroscopies), x-ray absorption spectroscopy is particularly powerful to obtain local information on the geometrical and

a)Electronic mail: denis.testemale@esrf.fr

electronic structure of any compound. Thus many studies using this tool have been dedicated to the structural characterization of the hydration of cations and anions of metals and nonmetallic elements at elevated pressure and temperature conditions.[2–20] Although the extended x-ray Absorption Fine Structure (EXAFS) analysis is widely used to get information on the structure of molecular aqueous complexes (see Ref. 21 and references therein), quantitative analysis of the x-ray Absorption Near Edge Structure (XANES) is rather new for aqueous systems. Recently, advances in this field have been made with the appearance of different codes based on the full multiple scattering scheme. For instance, Benfatto *et al.*[22] developed a code that has been used to model the geometry of ion hydration shells.[19,20] In the present study, we used another approach with the code FDMNES (Ref. 23) that calculates the absorption cross section beyond the muffin-tin approximation (realistic calculations). We show that such an approach is compulsory in the case of the nondense and asymmetrical structure of the aqueous $As(OH)_3$ molecule. Furthermore, an experimental cell has been developed that enables the acquisition of both transmission and fluorescence spectra of high quality for low concentration samples (absorber concentration $\leqslant 0.3m$): these conditions allow to reduce the solute-solute interactions that may exist between solute molecules.[24,25]

Section II describes briefly the experimental and analytical methods employed in the present study to collect and model the experimental and calculated x-ray absorption spectroscopy spectra. In Sec. III, we present the results of both EXAFS and XANES analyses. Finally, Sec. IV addresses the discussion concerning the relation between the evolution of the structure of $As(OH)_3$ and the properties of water itself at elevated conditions of pressure and temperature.

II. EXPERIMENTAL AND ANALYTICAL METHODS

A. Cell design and spectra acquisition

XAS spectra at the As *K* edge (11 867 eV) were obtained at the CRG-IF BM32 beamline at the European Synchrotron Radiation Facility (ESRF, Grenoble, France). This beamline is installed on a bending magnet (0.8 T). It is constituted by a parabolic Ni-coated mirror, a Si (111) double-crystal monochromator and an experimental setup for different XAS acquisition modes (transmission and fluorescence). The spot size ($200\times300\ \mu m^2$) is kept constant on the sample using the dynamical sagittal focusing of the second crystal of the monochromator.[26] The spectra were recorded at the As *K* edge in both transmission and fluorescence modes: the former through two Si diode detectors located above and below the sample on the x-ray beam and the latter with a 30 Ge elements Canberra detector.

The samples studied were $0.3m$ and $0.05m$ (moles per kg of solvent) arsenious acid aqueous solutions. They were prepared by dissolving As_2O_3 (Merck Normapur) in deionized water (18 MΩ) at 90 °C. The spectra were recorded at 250 and 600 bars and temperatures from 30 to 500 °C for the $0.3m$ As solutions, and at 250 bars and temperatures from 30 to 350 °C for the $0.05m$ sample.

A first EXAFS analysis of the $0.3m$ solutions was reported in Ref. 27. The cell used for these measurements has been described in detail elsewhere.[3,18,27–29] For the $0.05m$ samples, a High Pressure (HP)/High Temperature(HT) setup, designed recently in the Laboratoire de Cristallographie (CNRS-Grenoble), was used. It will be described in details in a further publication.[30] This cell design is compatible with many different x-ray based techniques (XAS in both transmission and fluorescence modes, small angle x-ray scattering, inelastic x-ray scattering, and visible Raman scattering, and it operates in a wide range of temperature and pressure ($T\leqslant600$ °C and $P\leqslant600$ bars for aqueous samples, and $T\leqslant1700$ °C and $P\leqslant2000$ bars for liquid metals and metallic glasses). In the present work, several scans have been recorded for each sample, both in transmission and fluorescence modes at the same time, at each pressure and temperature. Reversibility has been checked at each *T*-*P* point: the absorption jump at the As *K* edge, proportional to the sample density, was found to be perfectly reversible on increasing and decreasing temperature, as well as the shape of the XANES and EXAFS spectra.

B. EXAFS analysis procedure

The EXAFS data processing was conducted with a set of programs taken from the UWXAFS project.[31] This software allows to use the cumulants method[32] and take into account the multiple scattering contributions in the signal. The standard analysis procedure is followed. First, the EXAFS oscillations $\chi(k)$ are extracted by substraction of the baseline with the AUTOBK program;[33] the baseline is defined by the low *R* components in the Fourier transform of the above edge oscillating part of the spectra. Then, the analysis of these oscillations is performed with FEFF 8.0 and FEFFIT.[34,35] FEFF 8.0 calculates the scattering functions (amplitude and phase) and the mean free paths of single and multiple scattering paths within the structure of the cluster under consideration. The geometrical parameters of these paths (number *N* of oxygen neighbors, distance r_0 between As and O atoms and Debye–Waller parameter σ^2) are extracted by fitting the experimental spectra with FEFFIT.

C. XANES simulations

The XANES part of the absorption spectrum extends up to 50–60 eV beyond the threshold. It is known to be highly sensitive to the three-dimensional structural environment around the absorbing atom. Moreover, the photoelectron acting as a localized probe of the electronic environment, it is expected that XANES spectra will be sensitive to the evolution of the local charges with temperature. We used the FDMNES package,[23] which runs within the real space cluster approach. The absorption cross section is calculated optionally under two procedures:

(1) The first one uses the multiple scattering (MS) theory where the cross section is calculated in terms of path operators solving the Lippman–Schwinger equation. It uses the muffin-tin (MT) approximation for the shape of the potential where this one is spherically averaged in the atoms and constant between them.

TABLE I. Structural parameters of the first As coordination shell derived from EXAFS fits (reference As_2O_3 and As(III) aqueous samples from ambient up to supercritical conditions). The Fourier parameters are *k* weighting (3.8–11.5 Å) Hanning apodisation window, and (0.9–2.8 Å) real space fitting range. The reduction factor S_0^2 is deduced from a fit of the arsenolite reference spectra, and fixed to 0.83 for aqueous samples. (f) means the corresponding parameter is fixed during the fit. The goodness of the fits is considered via the *R* factor and the uncertainties are calculated through an inversion of the curvature matrix (Ref. 35) (numbers between brackets).

	ρ_{water} (g cm^{-3})	r_0 (Å)	N_0	σ^2(10^{-3} Å^2)	ΔE_0 (eV)	*R* factor
Arsenolite As_2O_3		1.787(*f*)	3(*f*)	1.9 (4.2)	10.7	0.004
		$As(OH)_3$, 0.3*m*, 250 bars				
30 °C	1.00	1.77 (0.01)	3.0 (0.2)	1.2 (0.9)	12.3 (1.1)	0.007
100 °C	0.97	1.77 (0.01)	3.0 (0.2)	1.6 (1.0)	12.3 (1.1)	0.007
200 °C	0.88	1.77 (0.01)	3.0 (0.2)	2.0 (1.1)	13.0 (1.2)	0.008
350 °C	0.63	1.77 (0.01)	3.0 (0.2)	2.6(*f*)	12.7 (1.4)	0.012
375 °C	0.51	1.76 (0.01)	3.0 (0.3)	2.8 (1.6)	11.0 (1.8)	0.016
425 °C	0.13	1.76 (0.01)	3.0 (0.3)	3.3 (1.6)	11.4 (1.7)	0.014
		$As(OH)_3$, 0.3*m*, 600 bars				
30 °C	1.02	1.77 (0.01)	3.0 (0.2)	1.2 (0.9)	12.6 (1.0)	0.007
100 °C	0.98	1.77 (0.01)	3.0 (0.2)	1.3 (0.9)	12.5 (1.0)	0.006
300 °C	0.79	1.77 (0.01)	2.9 (0.2)	1.7 (1.1)	12.5 (1.2)	0.008
375 °C	0.67	1.77 (0.01)	2.9 (0.2)	1.8 (1.0)	13.4 (1.2)	0.008
500 °C	0.34	1.78 (0.01)	2.9 (0.2)	2.5(*f*)	13.9 (1.4)	0.013
		$As(OH)_3$, 0.05*m*, 250 bars				
30 °C	1.00	1.75 (0.01)	3(*f*)	1.4 (0.5)	12.4 (1.1)	0.011
100 °C	0.97	1.75 (0.01)	3(*f*)	1.9 (0.5)	12.0 (1.3)	0.011
200 °C	0.88	1.75 (0.01)	3(*f*)	1.9 (0.6)	11.6 (1.4)	0.013
350 °C	0.63	1.76 (0.01)	3(*f*)	2.0 (0.6)	12.7 (1.5)	0.016
375 °C	0.51	1.76 (0.01)	3(*f*)	2.0 (0.6)	12.4 (1.6)	0.018

(2) The second procedure uses the finite difference method (FDM) to solve the Schrödinger equation. Its main advantage is the possibility to have a totally free potential shape, thus getting rid of the muffin-tin limitations.

Both procedures make further a Lorentzian energy-dependent convolution of the spectrum to account for the multielectronic and inelastic phenomena occurring in the absorption process. At the Fermi level, the Lorentzian width is due to both the interaction with the core hole and the monochromator resolution (respectively, 2.1 eV (Ref. 36) and about 2 eV at the As *K* edge on the interface beamline (IF) at ESRF). It was fixed at the total value of 3 eV full width at half maximum (FWHM) for photoelectron energy below 10 eV. For higher photoelectron energy, between 10 and 40 eV, the onset of plasmons collective interactions increase the Lorentzian width up to 7 eV. It is worth noting here that the same energy-dependent width was used in all the present XANES calculations.

The multiple scattering approach which uses the muffin-tin approximation is much less computer expensive than the FDM method. It is well suited for symmetrical and dense structures but is less satisfactory for highly asymmetrical or less dense structure found in many molecular species. In this case FDM method should be preferred as discussed thoroughly in Ref. 23. Nevertheless, MS calculations are performed first to assess the influence of the geometrical parameters on the spectra (defining the geometry of the cluster) and get a reasonable approximation. Then FDM calculations are conducted in order to specify the value and the evolution with temperature of the geometrical and electronic parameters. These geometrical parameters are the As-O distance, the O-As-O angle, and the location of the H atoms (i.e., As-O-H angle), which are expected to be of great importance despite their weak scattering power. Note that the As-O distance was first carefully evaluated by the EXAFS analysis (following section). The electronic parameters are the partial charges on the atoms (defined in terms of relative orbital occupancy of the As, O, and H atoms). Several models of partial charges were tested through the FDM calculations. It should be pointed that the inspection of charge evolution, by comparing experimental absorption spectra and realistic calculations, is an efficient method which has been developing for recent years in complicated chemical systems.[37,38] These local charges are found to be critical in the present case.

III. RESULTS

A. Results from EXAFS analysis

Several studies have shown that the +3 oxidation state of arsenic is stable in most high temperature hydrothermal fluids characterized by reducing conditions.[39–42] Available solubility and spectroscopic data indicate that the neutral hydroxide complex $As(OH)_3$ is the dominant species in both high density ($\rho > 0.4$ g cm^{-3}) and low density ($\rho < 0.4$ g cm^{-3}) hydrothermal fluids.[27,41,42] Under the assumption that individual and covalent $As(OH)_3$ species are largely dominant in solution,[27,42,43] a single shell model was used. The EXAFS parameters derived in this study are summarized in Table I. We checked the influence of including hydrogen atoms in the structure, but for the sake of brevity the corresponding results are not presented because they neither improved the fit nor altered it significantly. It stems from the fact that the hydrogen atoms show up in the EXAFS signal only when they are placed in focusing positions,[18,44–46]

which is not the case for the $As(OH)_3$ molecule. The influence of multiple scattering on the fit was also tested and found to be too weak to affect the structural parameters derived from single-shell fitting. All the results are in fair agreement with previous EXAFS works on identical arsenious acid solutions.[27,43,47]

The evolution of the value of σ^2 consists of a slight increase with temperature but its value remains low (from 1.2×10^{-3} Å^2 at 30 °C to 3.3×10^{-3} Å^2 at 425 °C 250 bars).[48] Neither the As-O distance nor the number of oxygen neighbors change with temperature and pressure within errors. The number of oxygen neighbors remains around 3 in the whole temperature range and the distance values are between 1.76 and 1.77 Å at 250 bars and between 1.77 and 1.78 Å at 600 bars. The 0.05*m* solutions are very close to those 0.3*m* solutions, except for the value of the As-O distance. Indeed, the mean value seems to be smaller (about 1.75 Å) for the 0.05*m* solutions (to be compared to the mean value of 1.77 Å for the 0.3*m* solutions).

B. Results from XANES analysis

1. Experimental spectra

The evolution of the XANES part of the experimental spectra as a function of temperature is presented in Fig. 1. In this figure, spectra are normalized to the density of water. It is worth identifying and describing the specific features of these spectra because the simulation part of the work will consist of reproducing them. The first obvious observation is the evolution of the white line with temperature: its intensity increases regularly while its position does not change at both pressures. The second point is the existence, at both pressures, of a resonance at about 8 eV above the threshold (indicated by the arrow on Fig. 1). The evolution of this feature with temperature is pressure independent: its amplitude is higher at 30 °C, rapidly decreases with increasing temperature, and becomes undetectable above 100 °C. Due to the low intensity of this feature above 200 °C, it is difficult to conclude about its evolution at higher temperatures. In Fig. 1, only three temperatures per pressure were drawn: 30 °C, 100 °C, and the higher temperature.

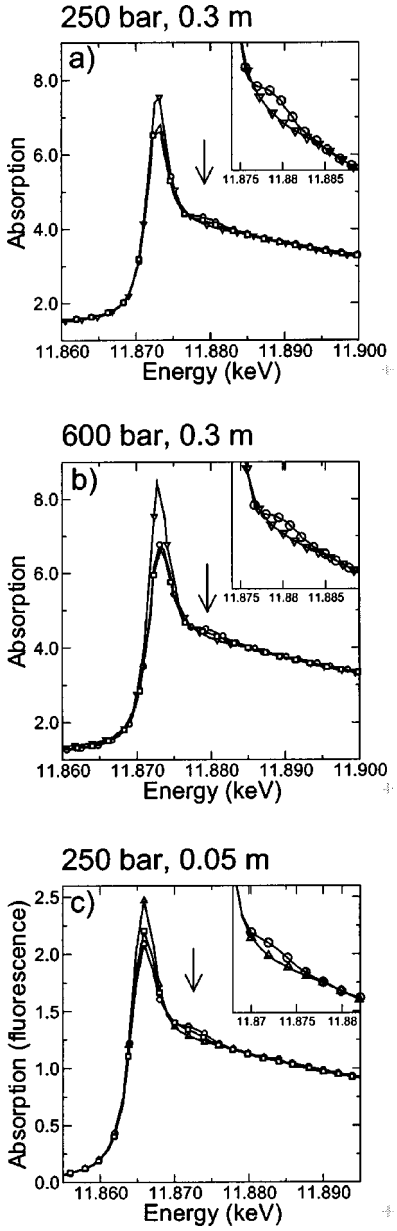

FIG. 1. Raw transmission XANES spectra of arsenious acid solutions (0.3*m*) (a) at 250 bars (30 °C, ○; 100 °C, □; 425 °C, ▽), (b) at 600 bars (30 °C, ○; 100 °C, □; 500 °C, ▽). (c) raw fluorescence XANES spectra of arsenious acid solutions (0.05*m*) at 250 bars (30 °C, ○; 100 °C, □; 375 °C, △). The spectra are scaled to the solvent density values. The vertical arrow denotes the resonance at 8 eV above the edge (see text). For reasons of clarity, only three temperatures are plotted. In the inset, the resonance region is plotted for the lowest and the highest temperature spectra.

2. XANES simulations

a. Muffin-tin Multiple Scattering (MT) versus *Finite Difference Method* (FDM). As it was already mentioned, the relevant geometrical parameters of our realistic XANES calculations are the O-As-O angle, the As-O distance, and the As-O-H angle. They need to be constrained to reasonable values by MS calculations (see Sec. II C). Determination of the structure of the $As(OH)_3$ cluster was recently derived from quantum mechanical *ab initio* calculations,[49,50] in agreement with Raman spectroscopy measurements.[24,42] These *ab initio* calculations predicted that the molecule has a pyramidal structure, with an apical arsenic atom and three OH groups at the basis, with an As-O distance around 1.75 Å, O-As-O angles between 97° and 99°, an O-H distance of 0.97 Å, and As-O-H angles about 120°. These angles coupled with the EXAFS mean As-O distance derived in the present study were a starting point for the MS muffin-tin calculations. By comparing these preliminary basic simulations with the experimental spectra in the EXAFS region, it appeared that these geometrical values were not far from reality, since they generate spectra similar to the experimental ones (amplitude and positions of the oscillations) in the (50–100 eV) range. For brevity these MS simulations are not detailed in this study. It is worth pointing out here that these MS muffin-tin calculations can only be considered as a first step. Indeed, the main experimental feature (the resonance 8 eV above the edge, see Fig. 1) can only be reproduced within FDM calculations, as it is demonstrated in Fig. 2. The inefficiency of the Muffin-tin approximation is due to the strong asymmetry of

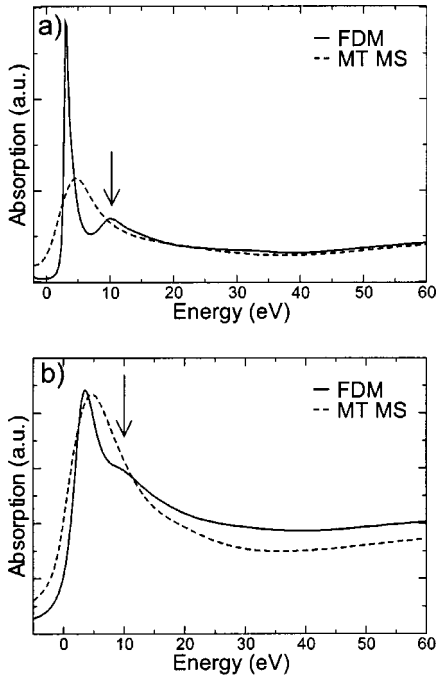

FIG. 2. (a) raw and (b) convoluted simulated spectra (distance As-O=1.77 Å, O-As-O=98°, As-O-H=120° and *E* charges, see Table II), within finite difference method FDM and Muffin-tin multiple scattering (MT MS) approaches.

the $As(OH)_3$ molecule and the very low energy position of the resonance considered (8 eV). Furthermore, still concerning the low energy part of the spectra, we shall pay attention to the good value of the convolution width, which was fixed *a priori* based on experimental and intrinsic considerations (see Sec. II C). This is visible in Fig. 3: the experimental and simulated spectra have the same white linewidth. Below, for the FDM calculations, we examine the influence of each parameter on the shape of the XANES simulated spectra and compare it with the experimental ones.

b. Atomic partial charges. The good order of magnitude of the atomic partial charges must be estimated first, in order to further vary the geometrical parameters. This estimation was done using FDM calculations within the same structure of $As(OH)_3$ as for the preliminary MS calculations: distance

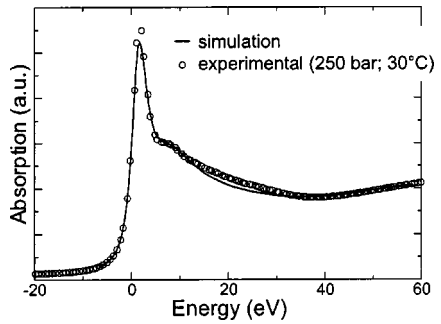

FIG. 3. Experimental spectrum (0.3 m; 250 bar; 30 °C) and FDM convoluted simulated spectrum (distance As-O=1.77 Å, O-As-O=98°, As-O-H =120°, *E* charges). The experimental spectrum is scaled to fit both the preedge and afteredge (−20)–(−5) eV and 40–60 eV regions, respectively). Note that the white line and the 8 eV feature are well reproduced in the calculated spectrum.

TABLE II. Values of the partial atomic charges on the atoms in the $As(OH)_3$ cluster. The Mulliken, AIM, and CHELPG sets of charges are calculated with the GAUSSIAN 98 package (Ref. 51).

Charge set	As	O	H
Mulliken charge values	+1.5	−0.65	+0.15
AtomsInMolecule charge values (AIM)	+1.83	−1.23	+0.62
CHELPG charge values	+0.48	−0.58	+0.42
"*Electronegativity*" charge values (refered to as "*E* charges")	+0.21	−0.34	+0.27
E charges ×1.5	+0.315	−0.51	+0.405
E charges ×2	+0.42	−0.68	+0.54

(As-O)=1.77 Å, angle (O-As-O)=98°, and angle (As-O-H) =120°. The different charges tested are displayed in Table II. The first two sets of partial charges (Mulliken and AIM) were obtained by *ab initio* quantum calculations within a Mulliken's population analysis (GAUSSIAN 98 program[51]). This type of charges was successfully used with FDMNES.[23] An additional set of charges, fitted to the electrostatic potential and the dipole of the cluster, was calculated with the CHELPG routine.[71] Finally, a set of lower charges, refered to as *electronegativity* charges in Table II, and labeled *E* elsewhere, was calculated on Sanderson's principle of balancing electronegativities[52] in the neutral cluster, using the electronegativity scale of Allred and Rochow.[53]

As it can be seen in Fig. 3, a very good agreement with the experimental spectrum is obtained with the *E* charges. Using either the Mulliken or the AIM charges, of the same order of magnitude, the convoluted spectra appeared to be very different from the experimental ones. The reason is that in the corresponding raw simulated spectra, i.e., before Lorentzian convolution, the white lines were systematically too low and too sharp to be discernible in the convoluted spectra (the white lines FWHMs were inferior to 1 eV whereas the width of the convoluting Lorentzian is 3 eV at the Fermi level). This is apparent in Fig. 4 which shows the raw simulated spectra, and the respective convoluted ones, for three different sets of charges: Mulliken, AIM, and *E* charges. One can see that the magnitude of the atomic charges affects significantly the amplitude, width, and position of the white line. However, the energy gap between the white line and the specific resonance is 8 eV in the three calculations, supporting the assumption that this feature is essentially related to geometrical parameters. It is worth noting, at this stage, that the *ab initio* quantum calculations with GAUSSIAN 98 are made for an isolated $As(OH)_3$ molecule in vacuum.

That is the reason why the Mulliken's charges (as well as the AIM charges), although successfully implemented in the FDMNES program,[23] are not appropriate in the present case. Indeed, the presence of the solvating environment around the covalent $As(OH)_3$ neutral complex influences strongly the magnitude of the partial charges, as compared to an isolated molecule. It is confirmed by the magnitude of the CHELPG charges, which are close to the *E* charges: the CHELPG charges are fitted to the electrostatic dipole of the isolated $As(OH)_3$ complex evaluated by the Hartree–Fock calculations; but this dipole value is always overestimated by this

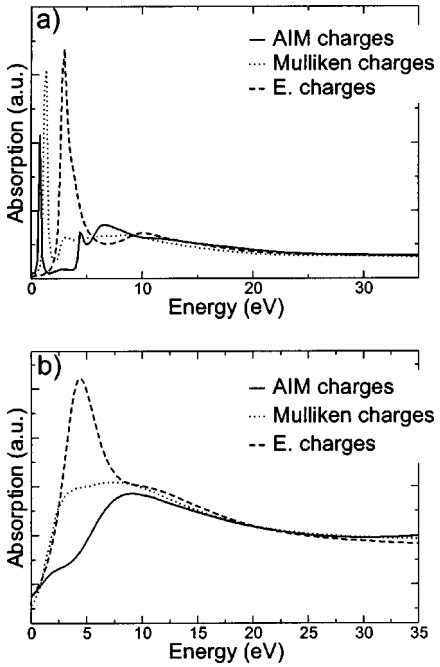

FIG. 4. (a) raw and (b) convoluted FDM simulated spectra (distance As-O =1.77 Å, O-As-O=98° and As-O-H=120°) for three different sets of charges (see Table II).

method[50] and can thus be considered closer to the real dipole value of nonisolated $As(OH)_3$ complex in its aqueous polarizable medium.

Once the right order of charges magnitude was determined, its influence on the spectra was investigated more precisely. In Fig. 5, three convoluted simulated spectra are plotted (O-As-O=98° and As-O-H=120°), corresponding to three different subsets of *E* charges: *E* charges, *E* charges ×1.5, and *E* charges ×2. Although the intensity of the white line in Fig. 5 diminishes with increasing the charges and its position is shifted regularly towards higher energy (a 1.7 eV shift between *E* charges and *E* charges ×2), it can be seen that the "8 eV" resonance is not modified by the charges magnitude (neither its amplitude, nor its position).

c. Hydrogen atoms positions. The hydrogen atoms can be placed in several configurations, defined by the distance O-H (kept fixed at 0.97 Å, see above) and the value of the As-O-H angle. For simplicity, it was assumed that all the

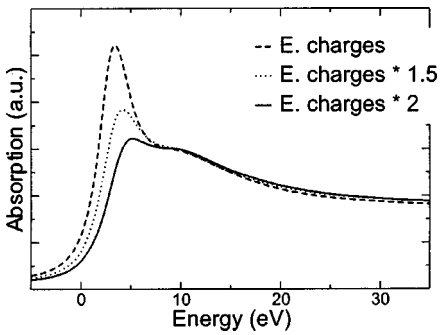

FIG. 5. Convoluted FDM simulated spectra (distance As-O=1.77 Å, O-As-O=98°, and As-O-H=120°) for three different set of charges: *E* charges, *E* charges ×1.5 and *E* charges ×2.

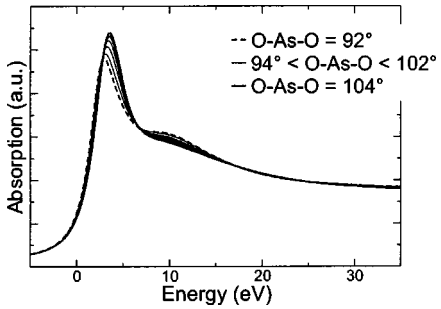

FIG. 6. Convoluted FDM simulated spectra (distance As-O=1.77 Å, As-O-H=120° and *E* charges) for O-As-O angles varying from 92° to 104° with a 2° step. For clarity, the 92° dashed line and the 104° solid line are shown in bold.

configurations conserve a symmetry C_{3V} for the $As(OH)_3$ cluster (all the bonds of the cluster belong to the three planes of symmetry). Keeping the O-As-O angle at 98° and the As-O distance at 1.77 Å, the As-O-H angle was varied from 180° (As, O, and H atoms aligned) to 120°. Figure 6 shows the resulting convoluted spectra. It appears that with increasing the As-O-H angle the resonance at 8 eV shrinks and the intensity of the white line increases. Both effects are similar to the experimental spectra evolution observed with increasing temperature (see Fig. 1). But the energy domain over which the simulated spectra do not superpose is much larger in Fig. 6 than in the experimental spectra in Fig. 1. In particular, between 20 and 30 eV above the white line, the simulated spectra are not similar, in contrast to the experimental spectra. Consequently, the evolution of the experimental spectra with temperature cannot be explained by an evolution of the hydrogen position. For this reason, in further simulations, it has been chosen to fix the As-O-H angle to 120°, the value resulting from the structure optimization using GAUSSIAN 98.[51] Our choice is reinforced by the good agreement between the experimental spectrum at ambient conditions and the simulated spectrum for O-As-O angle of 98° and As-O-H angle of 120° (see Fig. 3), and between experimental[42] and calculated[49] Raman frequencies for $As(OH)_3$ aqueous species with the same structure as used in the present study. However, it is worth noting the high sensitivity of the FDM simulated spectra to the position of H atoms, thus the small disagreement between experiment and simulation observed about 20 eV above the white line in Fig. 3 is most likely influenced by the H position (for example, twisting of the O-H bond out of the C_{3V} symmetry, or change of the O-H distance).

d. O-As-O *angle*. The spectra simulated with the set of *E* charges, for an As-O-H angle of 120° are plotted in Fig. 7 for various values of the O-As-O angle. Their comparison with the experimental spectra plotted in Fig. 1 shows that the evolution of the XANES features observed in the experiment with increasing temperature is similar to the changes in the simulated spectra with increasing the O-As-O angle. First, the white line intensity increases. Then, the amplitude of the resonance at 8 eV above the edge is reduced, and in contrast to what is observed when varying the hydrogen position, the rest of the spectra superposes perfectly. However, the varia-

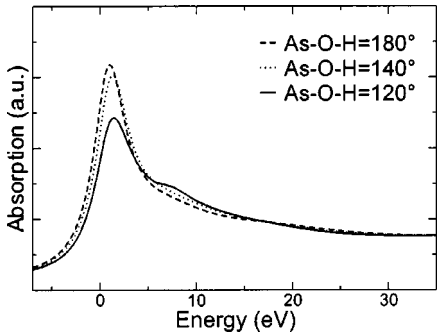

FIG. 7. Convoluted FDM simulated spectra (distance As-O=1.77 Å, O-As-O=98°, and *E* charges) for three different hydrogen positions (keeping the C_{3V} symmetry): As-O-H=180°, 140°, and 120°.

tion of the O-As-O angle has another effect, apparent in Fig. 7: the white line position shifts towards higher energies by about +0.5 eV when the O-As-O angles increases from 92° to 104°. Such an energy shift, large enough to be experimentally detected, is, however, not observed in the experimental spectra.

e. As-O *distance*. Since the solute concentration seems to affect the As-O distance (see Sec. III A), we checked the effect of varying this parameter on the XANES simulated spectra. Figure 8(a) shows the experimental XANES spectra of 0.3*m* and 0.05*m* arsenious acid solutions, at 30 and 375 °C. It is clearly visible that the amplitude of the white line is smaller at lower concentration. This effect is observed for all temperatures, and for both fluorescence and transmission spectra, ruling out any self-absorption effect[54] [fluorescence and transmission spectra of 0.05*m* solutions have been measured simultaneously and are identical, but for clarity reasons only fluorescence scans at two temperatures are plotted in Fig. 8(a)]. In Fig. 8(b), the corresponding simulated convoluted spectra are plotted. They correspond to two different distances (1.75 and 1.77 Å) for O-As-O angle=98° and As-O-H angle=120°. It appears that both spectra are similar (resonances shape and position), except for the intensity of the white line which is lower for the shorter distance. The comparison between experimental spectra and simulations leads to the conclusion that the As-O distance is smaller for the low concentration solutions. This XANES result reinforces the similar conclusion drawn from the EXAFS analysis.

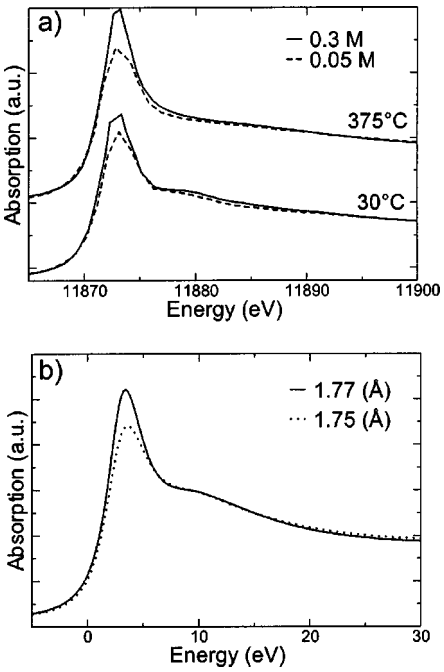

FIG. 8. (a) experimental XANES spectra for 0.3*m* and 0.05*m* arsenious acid solutions at 30 and 375 °C. (b) FDM convoluted simulated XANES spectra of the $As(OH)_3$ cluster with two As-O distances (1.75 and 1.77 Å).

IV. DISCUSSION

A. Covalent As-O bond

The EXAFS results of this study show that the radial structure of As environment in the neutral $As(OH)_3$ complex does not change within errors in a wide temperature (30–500 °C) and pressure (250–600 bar) range. This result is similar to existing studies dedicated to the evolution of the structure of strongly bonded metallic complexes of Mo and W in near-critical or supercritical aqueous solutions: WO_4^{2-} up to 400 °C in Ref. 9 and MoO_4^{2-} up to 150 °C in Ref. 55. The weak evolution with temperature of the value of σ^2 found for $As(OH)_3$ is also in agreement with those studies. Indeed, for the 0.3*m* samples, the σ^2 values vary from 1.2×10^{-3} Å^2 at 30 °C/250 bars to 3.3×10^{-3} Å^2 at 425 °C/250 bars and are of the same order of magnitude as in those works (for tungstate ions σ^2 increases from 1.5×10^{-3} Å^2 at 20 °C/1 bars to 2.2×10^{-3} Å^2 at 400 °C/450 bars,[9] and for molybdate ions[55] σ^2 values are around 5×10^{-3} Å^2). It is worth comparing these values to those found for hydrated ions in aqueous high temperature solutions[3–5,7,8,10,14,18] where the typical values of the Debye–Waller (DW) factor of the hydration shell are much higher. For monovalent ions, the DW factor is higher than 20×10^{-3} Å^2 [see for example Br^--H_2O (Refs. 3, 10, and 11), Cu^+-H_2O (Ref. 8), and Ag^+-H_2O (Ref. 14) shell parameters]. Due to a reinforcement of the coulombic interactions with charge of cations, the DW factor is smaller (but still remains much higher than that for $As(OH)_3$) for solvated divalent or trivalent metallic cations [around 8×10^{-3} Å^2 for Zn^{2+}-H_2O (Ref. 3), for Ni^{2+}-H_2O (Ref. 10) and for La^{3+}-H_2O (Ref. 4)]. Concerning the number of neighbors, no reduction of this parameter is observed at supercritical conditions for the $As(OH)_3$ molecule in water. This strongly suggests the absence of significant disorder in the As-O bond within the $As(OH)_3$ molecule, in contrast with what is observed in the EXAFS studies of ions hydration shells in such conditions.[5] These comparisons demonstrate the strong covalent character of the As-O bonding in the $As(OH)_3$ molecule, as it was stressed in Ref. 27. Besides, the present small variation of the DW factor with temperature can be interpreted in terms of molecular forces within the bond. In their study of the temperature dependence of the mean square displacement[56] Beni *et al.* report an analytical relation in which σ^2 is proportional to the temperature and to the inverse of the molecular force field term. Considering this relation, and the weak dependence of σ^2 upon temperature for the As-O shell, one can

conclude that the constant As-O distance found here is consistent with a strong covalent force in the As-O bond.

B. Evolution of intermolecular interactions

Because the $As(OH)_3$ molecule is neutral, the coulombic interactions with the dipoles of water molecules are limited. Hence, the existence of an outer hydration shell strongly bonded to the cluster is very improbable, thus explaining the high stability of the As-O distance when the water structure changes with increasing temperature. Nevertheless, as indicated in the introduction, the existence of three OH groups with hydrogen bonding affinity suggests the existence of hydrogen bonding association between the $As(OH)_3$ molecule and the solvent water molecules not detectable by EXAFS. Such an interaction is most likely to evolve in elevated conditions of temperature and pressure, having for consequence the modification of the internal structure of the molecule.

Based on comparisons between experimental and simulated spectra, XANES analysis leads to the conclusion that the O-As-O angle increases with increasing temperature. This increase starts between 30 and 100 °C and seems to stop above 200 °C. This is in agreement with previous Raman results.[24,42] In these studies, the authors measured the Raman signal from $As(OH)_3$ solutions at different concentrations. For the low concentration samples (0.02–0.5 mol kg^{-1}), the form of the spectra does not change in the temperature range 20–250 °C, except for a small shift (by a few cm^{-1}) of the two Raman bands ($a1$ and $a3$) towards lower wave numbers (cm^{-1}). Under the assumption that the molecule symmetry remains C_{3V} when the temperature is increased, a shift of the band towards low wave numbers can be explained by an increase of the angles.[57]

The ''opening'' of the $As(OH)_3$ cluster with temperature, below 200 °C, can be explained by a reduction of the interactions through H bonds between the complex $As(OH)_3$ and the water molecules. The cluster, which is constrained in the tetrahedral arrangement of water molecules at low temperature, is released when the temperature increases and the hydrogen bonds weaken. The electrostatic repulsive interactions between oxygen atoms of the $As(OH)_3$ molecule can thus result in the enlargement of the pyramidal structure, ending in a more symmetrical configuration (closer to a regular tetrahedron) consistent with the sp^3 hybridization of the outer electronic orbitals of the As atom. This conclusion based on structural analysis is also strongly supported by the evolution of the apparent hydration number of arsenious acid, derived from As_2O_3 solubility measurements in H_2O-inert organic compound solvents.[58] Thermodynamic predictions based on these data indicate that $As(OH)_3 \cdot 4H_2O$ is the dominant species in a water-rich solvent below 100 °C, but this complex is progressively replaced by $As(OH)_3$ with increasing temperature, showing the reduction of the interactions between the cluster $As(OH)_3$ and water molecules.

The reduction of the As-O distance in the low concentration solutions, determined by EXAFS analysis and confirmed by XANES modeling, cannot be explained at present. A possible interpretation is the existence of solute-solute interactions by hydrogen bonding interactions between the OH groups in the higher concentration solutions, that would lead to an elongation of the As-O distance.[24] But a systematic determination of this distance with varying the concentration should be made in order to confirm this effect. Recent EXAFS experiments on the germanic acid at hydrothermal conditions do not show the same tendency for the Ge-O distance in the $Ge(OH)_4$ complex. The Ge-O distance remains the same within 0.004 Å in a wide range of Ge concentrations ($0.02m-0.09m$).

C. Evolution of atomic charges

The XANES modeling carried out in this work predicts that the partial atomic charges in the $As(OH)_3$ complex may change with increasing temperature. Indeed, as it was demonstrated by the XANES analysis, the white line position in the experimental spectra does not change with increasing either T or P (see Fig. 1), which is in apparent disagreement with the small shift of this position caused by the variation of the O-As-O angle as predicted by XANES modeling (see Fig. 7). The evolution of the white line with increasing temperature can thus be interpreted by the competition between a widening of the O-As-O angle and a reduction of the atomic charges. Indeed, the former tends to increase the white line intensity and to shift it towards higher energy, and the latter also increases the white line intensity but shifts it towards lower energy. A counterbalance of both effects on the white line results in a global increase of its intensity while its position does not change, which is the experimental observation.

The weakening of the atomic partial charges is likely to stem from the decrease of hydrogen bonding at elevated temperature conditions. Indeed, the reduction of hydrogen bonding interactions between solvent molecules themselves is responsible for the decrease of the water permittivity (see next paragraph), resulting in the global reduction of the charges of the solute atoms immersed in the solvent. Furthermore, the joint reduction of hydrogen bonding interactions between water molecules and the OH groups of $As(OH)_3$, already responsible for the increase of the O-As-O angle (see above), may diminish the additional molecule polarizability, and hence the atomic charges of As, O, and H atoms.

D. Temperature dependence

As proposed just above, the structural and electronic evolution of $As(OH)_3$ is caused by the reduction of the hydrogen bonding interactions both between the OH groups of the molecules and the water molecules (modification of the local hydration) and between the water molecules themselves (resulting in the decrease of ϵ). It is thus interesting to observe if the temperature dependence of the modifications in $As(OH)_3$ is the same as the temperature dependence of hydrogen bondings and ϵ evolution.

The destruction of the tetrahedral arrangement of water molecules with increasing temperature is responsible for the decrease of the permittivity ϵ which collapses from 80 at ambient conditions down to 6 at the critical point, 374 °C 221 bars.[59–62] Indeed, the high value of ϵ at ambient conditions, compared to simple liquids, is explained, within the

Kirkwood theory,[63] by the dipole-dipole interaction term resulting from the hydrogen bonding association. Several studies have been dedicated to experimental estimation of water permittivity[60–62,64] and spectroscopic observation of hydrogen bonding in water (see Ref. 65 and references therein) at high temperature and pressure conditions. For example, the permittivity value $\epsilon(0)$, which is around 80 at ambient conditions, is about 40 at 200 °C, and about 20 at 300 °C, at pressures in the 100–500 bars range.[64] In the RMN study of Hoffmann and Conradi,[65] the authors measure the variation of the mean number of hydrogen bonds in subcritical and supercritical water. At 250 bars they found that, in comparison with room temperature, there are about 70% (60% and 45%) of hydrogen bonds at 100 °C (200 and 300 °C, respectively). Their results are in very good agreement with previous NMR and Raman measurements of hydrogen bonding. Those experimental studies also reveal a really weak pressure dependence at these low temperature/high density conditions. Many theoretical studies tend to support the experimental observations.[66–70] Jedlovsky and Richardi compare different water models' viability to reproduce water properties from ambient to supercritical conditions.[66] Concerning the permittivity value at HP/HT conditions, these calculations reveal, at 300 °C, a strong decrease of $\epsilon(0)$ to 1/4 the ambient value. In Ref. 69, a geometrical and topological study of the hydrogen-bonding structure, based on RMC calculations, indicates a notable modification of its tetrahedral arrangement from 150 °C upwards. It is thus evident that the hydrogen bonded network of water and the corresponding value of the permittivity rapidly evolve with increasing temperature mostly in the 30–200 °C range.

In our study, the increase of the O-As-O angle and the decrease of the atomic charges occur below 200 °C, and do not depend on pressure. That is in accordance with the rapid evolution of the solvent properties mentioned just above. For temperatures above 200 °C, changes in the XANES spectra become undetectable. This might imply that either the structural and electronic evolution of $As(OH)_3$ stops, or a further evolution of both angles and charges go on but is undetectable within the resolution of the methods. No unequivocal conclusion can be drawn at this point.

V. CONCLUSION

The structure of the $As(OH)_3$ covalent molecule in aqueous solutions was determined by X-Ray absorption spectroscopy from ambient to supercritical temperatures. Both EXAFS analysis and XANES simulations were used to obtain information on the evolution of the geometry of As environment (distances, angles) and its electronic configuration (atomic partial charges) with temperature and pressure. The EXAFS analysis shows the constancy of the As-O distance, which remains about 1.77 Å in 0.3*m* solutions in the whole temperature range 30–500 °C at 250 and 600 bars, and about 1.75 Å in 0.05*m* solutions in the temperature range 30–375 °C, at 250 bars. These new data confirm that the As-O bonding has a strong covalent character, which keeps up under the supercritical temperature conditions. New XANES simulations reveal an enlargement of the O-As-O angles when temperature increases, coupled with a small reduction of the atomic partial charges magnitude. The changes in the solvent structure, such as the weakening of the hydrogen bonded network concomitant with the decrease of the solvent dielectric constant, are invoked to explain the structural and electronic modifications in the $As(OH)_3$ cluster with increasing temperature: the interactions between the As hydroxide complexes and water molecules originating from hydrogen bonding weaken, thus releasing the molecule from the hydrogen bonded network. This release enables the molecule to open its structure to a more tetrahedrallike configuration consistent with the sp^3 hybridization of the As electronic orbitals. At the same time, the decrease of the bulk water permittivity justifies the reduction of the partial atomic charges. All these effects take place at both concentrations (0.3*m* and 0.05*m*) as soon as the temperature is increased, the major changes occuring between 30 and 200 °C. This is in agreement with several theoretical and experimental studies on water showing a strong reduction of its dielectric properties in this temperature range. The combination of EXAFS analysis with XANES realistic simulations is demonstrated to be a powerful tool to get precise information on both geometrical and electronic (partial charges) structures of aqueous complexes and on the solvent itself, in high temperature/high pressure fluids. This HP/HT study would not have been possible without the development of an efficient experimental setup that allows to obtain high-quality transmission and fluorescence spectra.[30]

ACKNOWLEDGMENTS

The authors thank J.-C. Soetens for his strong help with the various GAUSSIAN 98 calculations, and J.-M. Beny for the Raman calculations of the normal modes frequencies.

[1] A. G. Kalinichev, *Reviews in Mineralogy and Geochemistry* (Mineralogical Society of America, Washington, D.C., 2001), Vol. 42, p. 83.
[2] A. Filipponi, S. DePanfilis, C. Oliva, M. A. Ricci, P. D'Angelo, and D. T. Bowron, Phys. Rev. Lett. **91**, 165505 (2003).
[3] V. Simonet, Y. Calzavara, J.-L. Hazemann, R. Argoud, O. Geaymond, and D. Raoux, J. Chem. Phys. **117**, 2771 (2002).
[4] A. J. Anderson, S. Jayanetti, R. A. Mayanovic, W. A. Bassett, and I.-M. Chou, Am. Mineral. **87**, 262 (2002).
[5] G. Ferlat, A. S. Miguel, J. F. Jal, J. C. Soetens, P. A. Bopp, I. Daniel, S. Guillot, J. L. Hazemann, and R. Argoud, Phys. Rev. B **63**, 134202 (2001).
[6] J. L. Fulton, D. M. Pfund, S. L. Wallen, M. Newville, E. A. Stern, and Y. Ma, J. Chem. Phys. **105**, 2161 (1996).
[7] J. L. Fulton, M. M. Hoffmann, and J. G. Darab, Chem. Phys. Lett. **330**, 300 (2000).
[8] J. L. Fulton, M. M. Hoffmann, J. G. Darab, B. J. Palmer, and E. A. Stern, J. Phys. Chem. A **104**, 11651 (2000).
[9] M. M. Hoffmann, J. G. Darab, S. M. Heald, C. L. Yonker, and J. L. Fulton, Chem. Geol. **167**, 89 (2000).
[10] M. M. Hoffmann, J. G. Darab, B. J. Palmer, and J. L. Fulton, J. Phys. Chem. **103**, 8471 (1999).
[11] R. A. Mayanovic, A. J. Anderson, W. A. Bassett, and I.-M. Chou, Chem. Phys. Lett. **336**, 212 (2001).
[12] R. A. Mayanovic, A. J. Anderson, W. A. Bassett, and I.-M. Chou, J. Synchrotron Radiat. **6**, 195 (1999).
[13] D. M. Pfund, J. G. Darab, J. L. Fulton, and Y. Ma, J. Phys. Chem. **98**, 13102 (1994).
[14] T. M. Seward, C. M. B. Henderson, J. M. Charnock, and B. R. Dobson, Geochim. Cosmochim. Acta **60**, 2273 (1996).
[15] T. M. Seward, C. M. B. Henderson, J. M. Charnock, and T. Driesner, Geochim. Cosmochim. Acta **63**, 2409 (1999).
[16] S. L. Wallen, B. J. Palmer, D. M. Pfund, and J. L. Fulton, J. Phys. Chem. **101**, 9632 (1997).

[17] S. L. Wallen, B. J. Palmer, and J. L. Fulton, J. Chem. Phys. **108**, 4039 (1998).
[18] V. Simonet, Y. Calzavara, J.-L. Hazemann, R. Argoud, O. Geaymond, and D. Raoux, J. Chem. Phys. **116**, 2997 (2002).
[19] M. Benfatto, P. D'Angelo, S. DellaLonga, and N. V. Pavel, Phys. Rev. B **65**, 174205 (2002).
[20] P. D'Angelo, M. Benfatto, S. DellaLonga, and N. V. Pavel, Phys. Rev. B **66**, 064209 (2002).
[21] A. Filipponi, J. Phys.: Condens. Matter **13**, 23 (2001).
[22] M. Benfatto and S. DellaLonga, J. Synchrotron Radiat. **8**, 1087 (2001).
[23] Y. Joly, Phys. Rev. B **63**, 125120 (2001).
[24] R. Gout, G. S. Pokrovski, J. Schott, and A. Zwick, J. Raman Spectrosc. **28**, 725 (1997).
[25] Note that for such low concentrations, the acquisition of diffraction patterns $S(q)$ is impossible.
[26] J.-L. Hazemann, K. Nayouf, and F. D. Bergevin, Nucl. Instrum. Methods Phys. Res. B **97**, 547 (1995).
[27] G. S. Pokrovski, I. V. Zakirov, J. Roux, D. Testemale, J.-L. Hazemann, A. Bychkov, and G. Golikova, Geochim. Cosmochim. Acta **66**, 3453 (2002).
[28] Y. Soldo, J.-L. Hazemann, D. Aberdam, M. Inui, K. Tamura, D. Raoux, E. Pernot, J.-F. Jal, and J. D. Philon, Phys. Rev. B **57**, 258 (1998).
[29] K. Tamura, M. Inui, and S. Hosokawa, Rev. Sci. Instrum. **66**, 1382 (1995).
[30] D. Testemale, O. Geaymond, R. Argoud, and J.-L. Hazemann (unpublished).
[31] E. A. Stern, M. Newville, B. Ravel, Y. Yacoby, and D. Haskel, Physica B **208–209**, 117 (1995).
[32] G. Bunker, Nucl. Instrum. Methods Phys. Res. **207**, 437 (1983).
[33] M. Newville, P. Livins, Y. Yacoby, J. J. Rehr, and E. A. Stern, Phys. Rev. B **47**, 14126 (1993).
[34] A. L. Ankudinov, B. Ravel, J. J. Rehr, and S. D. Conradson, Phys. Rev. B **58**, 7565 (1998).
[35] M. Newville, B. Ravel, D. Haskel, J. J. Rehr, E. A. Stern, and Y. Yacoby, Physica B **208–209**, 154 (1995).
[36] M. O. Krause and J. H. Oliver, J. Phys. Chem. Ref. Data **8**, 329 (1979).
[37] Y. Joly, D. Cabaret, H. Renevier, and C. R. Natoli, Phys. Rev. Lett. **82**, 2398 (1999).
[38] Y. Joly, S. Grenier, and J. E. Lorenzo, Phys. Rev. B **68**, 104412 (2003).
[39] N. N. Akinfiev, A. V. Zotov, and A. P. Nikonorov, Geochem. Intl. **29**, 109 (1992).
[40] G. R. Helz, J. A. Tossel, J. M. Charnock, R. A. D. Pattrick, D. J. Vaughan, and C. D. Garner, Geochim. Cosmochim. Acta **59**, 4591 (1995).
[41] G. S. Pokrovski, S. Kara, and J. Roux, Geochim. Cosmochim. Acta **66**, 2361 (2002).
[42] G. S. Pokrovski, R. Gout, A. V. Zotov, J. Schott, and J.-C. Harrichoury, Geochim. Cosmochim. Acta **60**, 737 (1996).
[43] Y. Arai, E. J. Elzinga, and D. L. Sparks, J. Colloid Interface Sci. **235**, 80 (2001).
[44] P. D'Angelo, A. DiNola, M. Mangoni, and N. V. Pavel, J. Chem. Phys. **104**, 1779 (1996).
[45] B. Lengeler, Phys. Rev. Lett. **53**, 74 (1984).
[46] K. R. Wilson, J. G. Tobin, A. L. Ankudinov, J. J. Rehr, and R. J. Saykally, Phys. Rev. Lett. **85**, 4289 (2000).
[47] I. J. Pickering, R. C. Prince, M. J. George, R. D. Smith, G. N. George, and D. E. Salt, Plant Physiol. **122**, 1171 (2000).
[48] Debye-Waller parameters have been evaluated by Recursion-Method calculations performed within FEFF 8 program for an AsO_3 cluster: these calculations yield a 0.0017 (resp. 0.0022) value at 30 °C (resp. 300 °C). The small disagreement with our experimental determination (0.0012 and 0.0017 at respective temperatures) is due to the small k range that we used.
[49] J. A. Tossell, Geochim. Cosmochim. Acta **61**, 1613 (1997).
[50] J.-C. Soetens (private communication).
[51] M. J. Frisch, G. W. Trucks *et al.*, GAUSSIAN Inc. (2001).
[52] R. T. Sanderson, Science **114**, 670 (1951).
[53] J.-P. Jolivet, *De La Solution a L'axyde*, Savoirs Actuels (CNRS, Paris, 1994).
[54] This has been however checked by quantitative determination of the self-absorption effect by use of the FLUO software (FLUO:correcting XANES for self-absorption in fluorescence measurements) by Daniel Haskel, University of Washington. For 0.05m solutions of heavy arsenic atom in light water molecules matrix, the effect is found negligible.
[55] J. F. W. Mosselmans, P. F. Schofield, J. M. Charnock, C. D. Garner, R. A. D. Pattrick, and D. J. Vaughan, Chem. Geol. **127**, 339 (1996).
[56] G. Beni and P. M. Platzman, Phys. Rev. B **14**, 1514 (1976).
[57] J.-M. Beny (ISTO-CNRS) made calculations of the normal Raman modes of the molecule AsF_3, analogous to $As(OH)_3$ and showed that an opening of the molecule results in a shift of the $a1$ band towards lower wavenumbers.
[58] G. S. Pokrovski, J.-M. Beny, and A. V. Zotov, J. Solution Chem. **28**, 1307 (1999).
[59] E. U. Franck, *The Physics and Chemistry of Aqueous Ionic Solutions* (Reidel, Dordrecht, 1987).
[60] D. G. Archer and P. Wang, J. Phys. Chem. Ref. Data **19**, 371 (1990).
[61] D. P. Fernandez, Y. Y. Mulev, A. R. Goodwin, and J. M. H. Sengers, J. Phys. Chem. Ref. Data **24**, 33 (1995).
[62] M. Uematsu and E. U. Franck, J. Phys. Chem. Ref. Data **9**, 1291 (1980).
[63] H. Fröhlich, *Theory of Dielectrics* (Oxford University Press, London, 1958).
[64] K. Okada, Y. Imashuku, and M. Yao, J. Chem. Phys. **107**, 9302 (1997).
[65] M. M. Hoffmann and M. S. Conradi, J. Am. Chem. Soc. **119**, 3811 (1997).
[66] P. Jedlovszky and J. Richardi, J. Chem. Phys. **110**, 8019 (1999).
[67] B. D. Bursulaya and H. J. Kim, J. Chem. Phys. **110**, 9646 (1999).
[68] Y. Guissani and B. Guillot, J. Chem. Phys. **98**, 8221 (1993).
[69] P. Jedlovszky, J. P. Brodholt, F. Bruni, M. A. Ricci, A. K. Soper, and R. Vallauri, J. Chem. Phys. **108**, 8528 (1998).
[70] A. K. Soper, F. Bruni, and M. A. Ricci, J. Chem. Phys. **106**, 247 (1996).
[71] C. M. Breneman and K. B. Wiberg, J. Comput. Chem. **11**, 361 (1990).